

Anomalous scaling of spin accumulation in ferromagnetic tunnel devices with silicon and germanium

S. Sharma^{1,2}, A. Spiesser¹, S. P. Dash³, S. Iba¹, S. Watanabe^{1,4}, B. J. van Wees², H. Saito¹, S. Yuasa¹ and R. Jansen¹

¹ *National Institute of Advanced Industrial Science and Technology (AIST), Spintronics Research Center, Tsukuba, Ibaraki 305-8568, Japan.*

² *Zernike Institute for Advanced Materials, Physics of Nanodevices, University of Groningen, 9747 AG, Groningen, The Netherlands.*

³ *Department of Microtechnology and Nanoscience, Chalmers University of Technology, SE-41296, Göteborg, Sweden.*

⁴ *University of Tsukuba, Tsukuba, Ibaraki 305-8571, Japan*

The magnitude of spin accumulation created in semiconductors by electrical injection of spin-polarized electrons from a ferromagnetic tunnel contact is investigated, focusing on how the spin signal detected in a Hanle measurement varies with the thickness of the tunnel oxide. An extensive set of spin-transport data for Si and Ge magnetic tunnel devices reveals a scaling with the tunnel resistance that violates the core feature of available theories, namely, the linear proportionality of the spin voltage to the injected spin current density. Instead, an anomalous scaling of the spin signal with the tunnel resistance is observed, following a power-law with an exponent between 0.75 and 1 over 6 decades. The scaling extends to tunnel resistance values larger than $10^9 \Omega\mu\text{m}^2$, far beyond the regime where the classical impedance mismatch plays a role. This scaling is incompatible with existing theory for direct tunnel injection of spins into the semiconductor. It also demonstrates conclusively that the large spin signal does not originate from two-step tunneling via localized states near the oxide/semiconductor interface. Control experiments on devices with a non-magnetic metal (Ru) electrode, instead of the semiconductor, exhibit no Hanle spin signal, showing that spin accumulation in localized states within the tunnel barrier is also not responsible. Control devices in which the spin current is removed by inserting a non-magnetic interlayer exhibit no Hanle signals either, proving that the spin signals observed in the standard devices are genuine and originate from spin-polarized tunneling and the resulting spin accumulation. Altogether, the scaling results suggest that the spin signal is proportional to the applied bias voltage, rather than the (spin) current.

I. INTRODUCTION

Mainstream semiconductors such as silicon and germanium play a key role in the development of a spintronics information technology in which spin is used to represent digital data¹⁻⁴. To create and detect spin-polarized carriers in non-magnetic materials, the use of ferromagnetic tunnel contacts has proven to be a robust and technologically viable approach that is widely used in spin-based devices, including those with Si and Ge⁵⁻²². As recently reviewed^{4,23}, controversy has arisen because in many semiconductor spintronic devices, the magnitude of the observed spin voltage differs by several orders of magnitude from what is expected based on the available theory for spin injection and diffusion²⁴⁻²⁷. A common feature of all theories is that the injected spin current produces a spin accumulation $\Delta\mu$, i.e., a spin splitting in the electrochemical potential and thus a spin-dependent occupation of the electronic states in the non-magnetic material. Conservation of spin-angular momentum requires the injected spin current to be balanced by spin relaxation, from which the steady-state non-equilibrium spin accumulation is evaluated. Consequently, the spin accumulation is predicted to be linearly proportional to the injected spin current.

A powerful way to test the predictions is to vary the thickness of the tunnel barrier, which changes the current density J exponentially. The spin accumulation is expected to exhibit a similar exponential variation, so that $\Delta\mu/J$ remains constant. Here we present an extensive set of spin-transport data on Si and Ge based magnetic tunnel devices with different tunnel oxides. The scaling of the detected spin voltage with tunnel oxide thickness violates the expected linear proportionality of spin voltage and injected spin current. The data is shown to be incompatible with any of the known theories, including those based on direct tunneling²⁴⁻²⁷ or two-step tunneling via localized states^{28,29}.

II. DEVICE FABRICATION

To illustrate the generic nature of the observed scaling, we use devices with heavily doped Si (p-type and n-type) as well as p-type Ge, with an amorphous Al_2O_3 tunnel barrier and $\text{Ni}_{80}\text{Fe}_{20}$ ferromagnet, or with epitaxial, crystalline MgO/Fe contacts. Tunnel contacts on Si(001) surfaces were fabricated using *n*-type silicon-on-insulator wafers with a $5 \mu\text{m}$ thick active Si layer having As-doping and a resistivity of $3 \text{ m}\Omega\text{cm}$ at 300 K, or *p*-type silicon-on-insulator wafers with a $3 \mu\text{m}$ thick active Si layer having B-doping and a resistivity of $11 \text{ m}\Omega\text{cm}$ at 300 K. For the contacts with

amorphous Al_2O_3 , the Si substrate was treated by hydrofluoric acid to remove oxide, the substrate was introduced into the ultrahigh vacuum chamber, and the tunnel barrier was prepared by electron-beam deposition of Al_2O_3 from a single-crystal Al_2O_3 source, followed by plasma oxidation for 2.5 minutes, and electron-beam deposition of the ferromagnetic-metal top electrode (typically 10 nm thick) and a Au cap layer, all at room temperature. For some devices (appendix A) the plasma oxidation step was omitted. The plasma oxidation leads to the formation of some additional silicon oxide. The actual tunnel oxide thickness is thus slightly larger than the nominal thickness of the deposited Al_2O_3 , as previously confirmed and quantified³⁰ by transmission electron microscopy (TEM). Values of the tunnel oxide thickness quoted in this manuscript correspond to the corrected, actual oxide thickness extracted from TEM, and for convenience this is referred to as the Al_2O_3 thickness.

For epitaxial contacts³¹ with MgO/Fe, after treatment with buffered hydrofluoric acid, the Si substrate was annealed in the ultrahigh vacuum deposition system to 700°C for 10 minutes to obtain a 2×1 reconstructed Si surface. The MgO tunnel barrier and the Fe electrode (10 nm thick) were deposited at 300°C and 100°C, respectively, and the crystalline nature of the layers was confirmed by *in situ* reflection high-energy electron diffraction and by high-resolution TEM, as reported recently³¹. Tunnel devices on p-type Ge(001) were prepared using Ga-doped wafers with a resistivity of 3 m Ωcm and a carrier concentration of $8.2\times 10^{18}\text{ cm}^{-3}$ at 300 K. The preparation of the epitaxial MgO/Fe tunnel contacts on Ge was as previously described²¹.

To probe the spin accumulation over a large range of the tunnel barrier thickness, we employ three-terminal devices⁷ in which a single ferromagnetic tunnel contact is used to inject the spin accumulation, and to detect it. This geometry, unlike 4-terminal non-local devices^{6,10}, allows the contact area to be chosen arbitrarily large so as to adjust the overall device resistance and thereby ensure a sufficient signal to noise ratio. Here, the tunnel junction area is between $10\times 10\ \mu\text{m}^2$ and $100\times 200\ \mu\text{m}^2$. Positive voltage corresponds to electrons tunneling from ferromagnet to semiconductor.

III. SCALING WITH TUNNEL BARRIER THICKNESS

In all devices, voltage signals corresponding to the Hanle and inverted Hanle effect³² were detected when a magnetic field is applied perpendicular or parallel to the tunnel interface, respectively, at constant tunnel current (Fig. 1). The Hanle (inverted Hanle) signal originates from the suppression (recovery) of the spin accumulation due to spin precession (or the reduction thereof), and is the signature of the presence of a spin accumulation^{7,32}. The most striking observation is that the amplitude of the spin signal (the spin RA product, defined as $\Delta V_{\text{Hanle}}/J$, the spin voltage signal per unit of J) increases by orders of magnitude when the thickness of the tunnel barrier is increased. The width of the Hanle curve and the ratio of the Hanle and inverted Hanle amplitudes are also not constant.

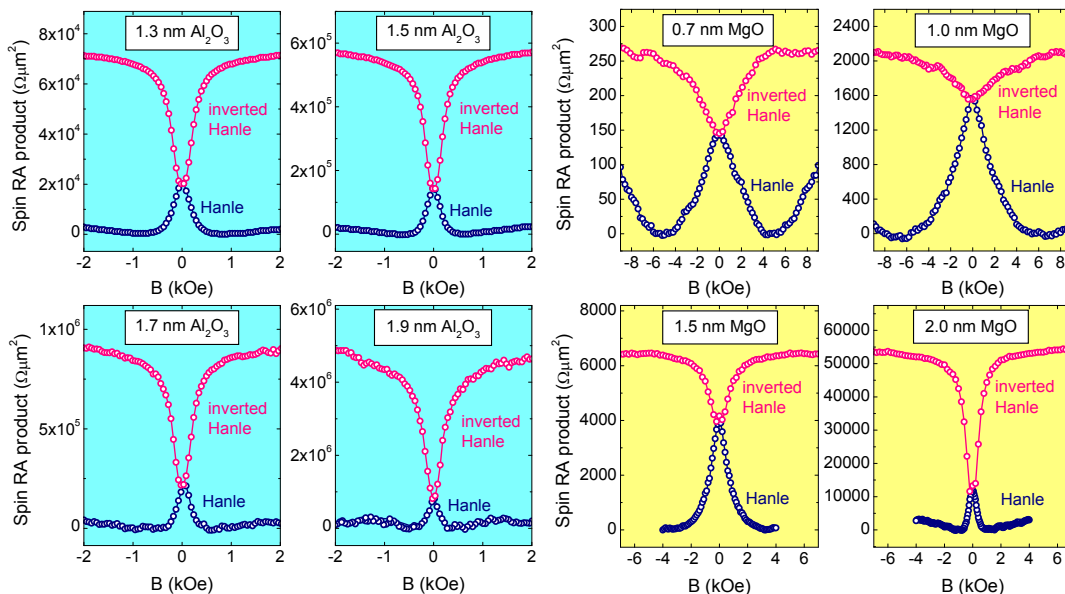


FIG. 1: Hanle detection of spin accumulation in semiconductor/oxide/ferromagnet tunnel devices. Shown are representative Hanle and inverted Hanle curves for magnetic field B applied, respectively, perpendicular or parallel to the magnetization of the ferromagnet. Data is shown for p-type Si/ Al_2O_3 / $\text{Ni}_{80}\text{Fe}_{20}$ and p-type Si/MgO/Fe devices with different thickness of the tunnel barrier, all at 300 K. The vertical axis gives the spin-RA product, defined as $\Delta V_{\text{Hanle}}/J$.

The tunnel resistance exhibits the expected exponential variation with thickness of the tunnel oxide (Fig. 2a). From the slope we extract an effective tunnel barrier height Φ_{eff} of 0.8 eV. Taking into account the effective electron mass in Al_2O_3 (about 0.2 - 0.3 times the free electron mass), this translates into a real barrier height of $\Phi = 3.2 \pm 0.8$ eV. This is a reasonable value³³ for Al_2O_3 on p-type Si, showing that direct tunneling from the ferromagnet into the Si is the dominant transport process (for multi-step tunneling via localized states within the oxide³⁴, the extracted barrier height would be 4 times larger, which is unrealistic). More importantly, the data implies that the contact resistance is dominated by the Al_2O_3 , and that the depletion region associated with the Schottky barrier in the Si contributes little to the resistance, as expected for heavily doped Si.

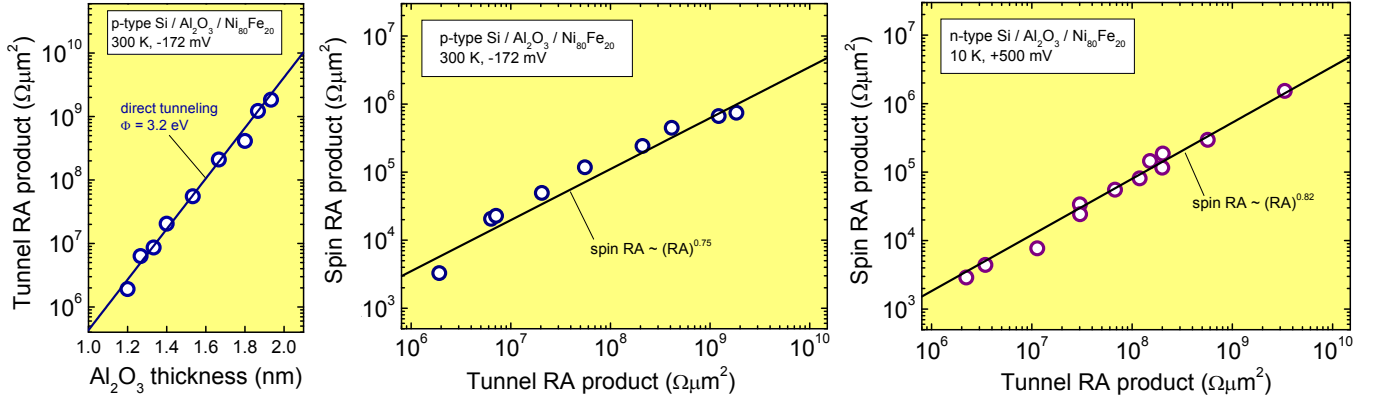


FIG. 2: Scaling of Hanle spin signals in Si tunnel devices with amorphous Al_2O_3 barrier. (a), tunnel resistance-area (RA) product versus Al_2O_3 thickness for p-type Si/ Al_2O_3 / $\text{Ni}_{80}\text{Fe}_{20}$ devices at 300 K. The extracted tunnel barrier height is 3.2 eV. (b), the corresponding spin RA product versus tunnel RA product. The solid line corresponds to a power law with exponent 0.75. (c), data for similar devices but with n-type Si at 10 K. The solid line corresponds to a power law with exponent 0.82. The spin RA value is derived from the Hanle signal only, instead of the sum of the Hanle and inverted Hanle signals. See appendix A for additional data with different oxidation time (p-type) and Cs treated surfaces (n-type).

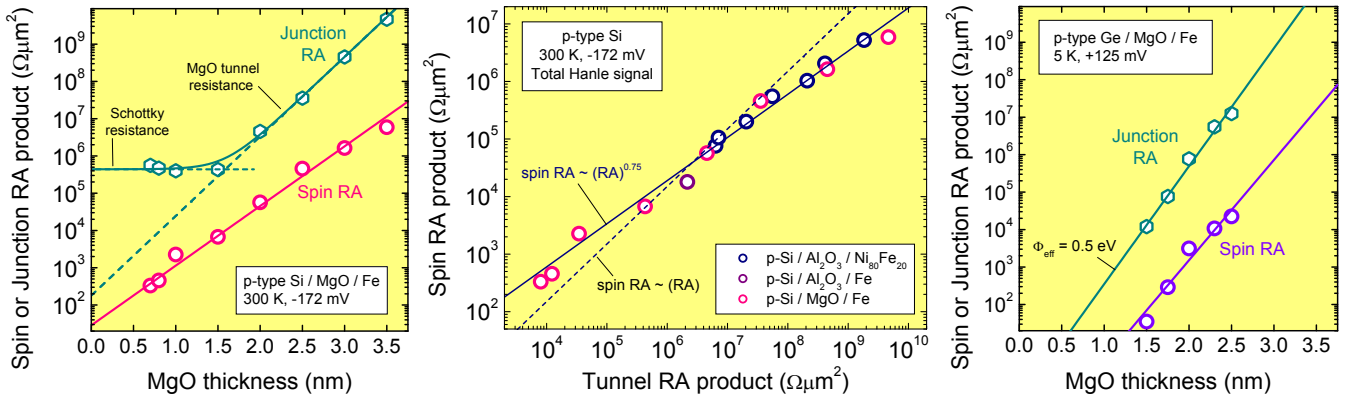


FIG. 3: Scaling of Hanle spin signals for devices with MgO and p-type Si or Ge. (a), spin RA product and tunnel RA product versus MgO thickness for p-type Si/MgO/Fe devices at 300 K. (b), corresponding spin RA product versus tunnel RA product for the same devices (pink symbols), together with data for p-type Si/ Al_2O_3 / $\text{Ni}_{80}\text{Fe}_{20}$ (blue symbols). For the 3 devices with the thinnest MgO barrier, the tunnel RA product is determined by extrapolation from the high thickness regime (dashed green line in a) to remove the Schottky resistance. The solid line corresponds to a power law with exponent 0.75. (c), data for p-type Ge/MgO/Fe devices at 5 K. The spin RA product is the sum of the Hanle and inverted Hanle signal.

The spin RA product also displays an exponential variation with thickness of the tunnel oxide, and a power law is revealed when the spin RA product is plotted against tunnel resistance (Figs. 2b and 2c). The associated scaling exponent is about 0.75 and 0.82, respectively, for Si/ Al_2O_3 / $\text{Ni}_{80}\text{Fe}_{20}$ devices with p-type and n-type Si. For devices with crystalline MgO/Fe contacts, a similar exponential variation of spin RA product with MgO thickness is obtained (Fig. 3a). The contact resistance is dominated by tunneling through the MgO at larger thickness, but for small MgO thickness a transition occurs to the regime where the contact resistance is limited by the Schottky barrier and becomes constant. Interestingly, the spin RA product displays no transition. It scales with the MgO thickness even

in the low thickness regime, suggesting that the spin signal is determined by the tunneling across the MgO. The spin RA products for p-type Si with MgO/Fe and Al₂O₃/Ni₈₀Fe₂₀ contacts display similar scaling as a function of resistance of the tunnel oxide (Fig. 3b), with an exponent (0.75) smaller than 1. For devices on heavily doped p-type Ge with crystalline MgO/Fe contacts^{20,21}, we also find that R_{tun} and the spin RA product vary exponentially with MgO thickness (Fig. 3c), although the data set is too limited to extract an accurate value for the scaling exponent. Note that a similar scaling was recently reported by Uemura *et al.* for n-type Si/MgO/Co₅₀Fe₅₀ devices³⁵, although a direct comparison cannot be made because their data was taken with the same bias current for each oxide thickness, and hence with a different tunnel voltage. This, in turn, changes the tunnel spin polarization, which is known to vary with the energy of the tunnel electrons^{36,37}. This additional source of variation of the spin signal with tunnel oxide thickness is not present in our data, which was obtained using the same bias voltage for each oxide thickness. Our collection of data leads to the striking and unexpected conclusion that $\Delta V_{Hanle}/J$ is not a constant but scales with R_{tun} , and up to values larger than $10^9 \Omega\mu m^2$. This behavior is generic, as it is observed for devices with different semiconductors, tunnel oxides, and ferromagnetic electrodes. Below we explain that this behavior is incompatible with any of the known theories for the injection, accumulation and diffusion of spins in ferromagnetic tunnel devices.

IV. COMPARISON WITH EXISTING THEORY

A. Direct tunneling

In the standard theory, the spin accumulation gives rise to a Hanle spin signal $\Delta V_{Hanle} = [P_{fm}^2] r_s J$, where P_{fm} is the tunnel spin polarization associated with the oxide/ferromagnet interface, and r_s is the spin resistance of the semiconductor^{23,38} that describes the relation between spin current and spin accumulation in non-magnetic materials. Thus, $\Delta V_{Hanle}/J$ is constant and independent of the resistance R_{tun} of the tunnel contact. This applies when R_{tun} is larger than r_s . If $R_{tun} < r_s$, back flow of the spins into the ferromagnet limits the spin signal^{23,24,38}, which is then proportional to the tunnel resistance: $\Delta V_{Hanle}/J = [P_{fm}^2/(1 - P_{fm}^2)] R_{tun}$. Although this produces a scaling with tunnel resistance, the experimentally observed scaling extends to tunnel RA values beyond $10^9 \Omega\mu m^2$, and a value of r_s larger than this would be required for back flow to be active. This is unreasonable, since r_s is typically around 10-100 $\Omega\mu m^2$ for the semiconductors used²³. The standard description thus predicts that $\Delta V_{Hanle}/J$ is independent of R_{tun} (and up to 7 orders of magnitude smaller than observed) and cannot describe the data.

B. Two-step tunneling

Two-step tunneling via localized states near the oxide/semiconductor interface can produce an enhanced spin signal due to spin accumulation in those states²⁸, provided that certain conditions are satisfied²³. To obtain a spin resistance of $10^9 \Omega\mu m^2$, localized states with a spin lifetime of at least 10 μs are needed for a reasonable density of interface states ($> 10^{12}$ states/eVcm²). While this cannot be excluded a priori, there exists ample experimental evidence that shows that this mechanism is not the origin of the large spin signals observed, as recently reviewed^{4,23}. The scaling data presented here provides additional and conclusive proof that two-step tunneling via interface states cannot be responsible, as it leads to a fundamental inconsistency. The scaling of the contact resistance with oxide thickness (Fig. 2a) implies that the resistance is dominated by the oxide tunnel barrier, and that any resistance r_b of the Schottky barrier in the semiconductor is much smaller. For two-step tunneling, the effective spin resistance r_s^{eff} of the interface states cannot be larger than the resistance r_b that couples the states to the bulk semiconductor^{23,28}. Taken together this would mean $r_s^{eff} < r_b < R_{tun}$. However, in order to obtain a scaling of the spin RA with tunnel resistance (due to back flow from the interface states into the ferromagnet), one needs the opposite, namely, $R_{tun} < r_s^{eff}$. These requirements cannot be satisfied simultaneously, whatever the parameters chosen. Thus, Tran's model²⁸ for spin accumulation in interface states is inconsistent with the simultaneous exponential scaling of contact resistance and spin signal with tunnel barrier thickness.

C. Two-step and direct tunneling in parallel

The model introduced by Tran *et al.*²⁸ for two-step tunneling via localized states assumes that *all* the current goes via the localized states and, as just noted, this cannot describe the experimental data. However, Tran's model has recently been extended²⁹ by including charge and spin transport by direct tunneling, in parallel with two-step tunneling. It is therefore important to examine whether this extended transport model can describe the experimental

data. Depending on the details of the system, the spin accumulation created in localized states due to two-step tunneling can be much larger than that induced in the semiconductor bands by direct tunneling. If as a function of some parameter (e.g. the tunnel barrier thickness) the relative contribution of two-step and direct tunneling is changed, then a transition from a small signal (direct tunneling dominant) to a large signal (two-step tunneling dominant) or vice versa, can be produced. In this paragraph we examine whether this can explain the observed scaling of the spin RA product with tunnel barrier thickness, and show that this is not possible.

We start by attempting to fit the experimental data for the p-type Si/MgO/Fe devices by setting the direct tunnel current to zero. That is, we consider transport by two-step tunneling, where the first step is by tunneling across the MgO from ferromagnet into interface states, and the second step is by tunneling through the Schottky barrier from interface states into the bulk semiconductor. The result is shown in the left two panels of Fig. 4, for which the spin resistance of the localized states was set to infinity, so that the spin signal is not limited by spin relaxation in the localized states. A good fit (thick solid lines) is obtained for the junction resistance. For small MgO thickness, the junction resistance is limited by the resistance of the Schottky barrier, whereas at large MgO thickness it is limited by tunneling across the MgO. According to the model, this should be accompanied by a transition in the behavior of the spin RA product, which first increases with MgO thickness, but becomes constant as soon as the junction resistance is determined by the MgO. This corroborates the statement made in the previous paragraph that the junction resistance and spin resistance cannot simultaneously exhibit a scaling with MgO thickness if transport is by two-step tunneling via localized interface states. Note that in the regime of small MgO thickness, the magnitude of the spin signal is determined by the tunnel spin polarization P_{fm} associated with the Fe/MgO interface, and a value of 20% is needed to obtain a match with the data in this regime. With a value of 75%, which is more reasonable³⁹, the data cannot be described, not even in the regime of small MgO thickness.

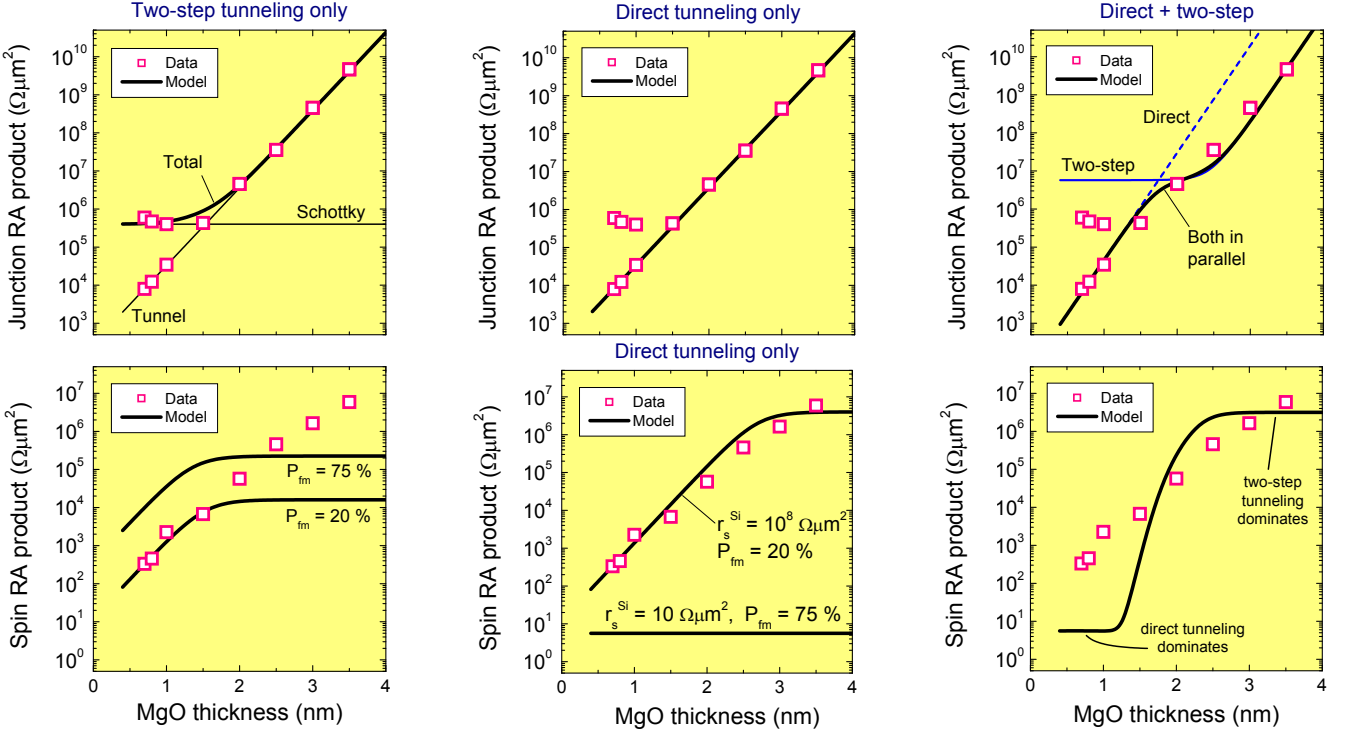


FIG. 4: Attempts to fit the data by direct and two-step tunneling in parallel. The experimental data (pink symbols) for the junction resistance and spin RA product of p-type Si/MgO/Fe devices is compared with the model (solid lines) for three cases: (i) two-step tunneling only, (ii) direct tunneling only, and (iii) two-step tunneling and direct tunneling in parallel. In the top panels, two data points are given for the junction RA product of the three junctions with smallest MgO thickness; the larger value corresponds to the measured junction RA product, whereas the smaller value is obtained when the resistance of the Schottky barrier is subtracted.

The two middle panels show the result if transport is purely by direct tunneling, setting the two-step tunnel current to zero. In principle the data can be described, however, the required spin resistance r_s^{Si} of the silicon is of the order of $10^8 \Omega\mu\text{m}^2$. This is unreasonable considering that is expected to be in the range of 10 - 100 $\Omega\mu\text{m}^2$ at best, for which one would obtain a spin RA product that is independent of the tunnel oxide thickness and orders of magnitude smaller than experimentally observed.

Next, we attempt to describe the data by direct and two-step tunneling in parallel, using the equations given in Ref. 29. As already eluded to above, in order to obtain an increase of the spin RA product as a function of MgO thickness, one needs to have a transition from transport dominated by direct tunneling to transport dominated by two-step tunneling via interface states. Such a situation is depicted in the two right panels of Fig. 4. At large MgO thickness, transport is determined by tunneling across the MgO, and we have chosen the parameters such that in this regime the resistance associated with two-step tunneling is smaller than that for direct tunneling. At small MgO thickness, the two-step tunnel current is limited by the resistance of the Schottky barrier. As a result, the transport at small MgO thickness is dominated by direct tunneling. This change in transport process can reasonably well describe the observed scaling of the junction resistance, but not the scaling of the spin signal. A transition from a small spin RA product, governed by direct tunneling, to an enhanced spin RA product due to two-step tunneling is indeed created, but the model does not reproduce the experimental data. It does not reproduce the observed exponential increase of the spin RA with MgO thickness, and deviates from the data in almost the entire range. We conclude that a transition in transport from direct to two-step tunneling does not describe the experimental data.

D. Inhomogeneous tunnel current density

It has previously been pointed out that an enlarged spin signal can be produced in three-terminal devices if the tunnel current density is not homogeneous across the contact area⁷. In that case the local current density, and thereby the spin accumulation, can be significantly larger than what is expected from the applied current and the lateral dimensions of the tunnel contact. In previous work⁷ the spin signal was larger than expected by 2-3 orders of magnitude and in principle this could be due to lateral inhomogeneity of the tunnel current. However, the new data presented here exhibit a scaling with tunnel barrier resistance that is not readily understandable with an explanation in terms of current inhomogeneity. Moreover, for devices with the thickest tunnel barrier, the observed spin signals are larger than expected by up to 6 orders magnitude, and this cannot be explained by inhomogeneous tunnel current. It would require that all the tunnel current goes via an area that is 10^6 times smaller than the geometric contact area of $100 \times 200 \mu\text{m}^2$. This translates into an effective tunnel area of only $100 \times 200 \text{nm}^2$ or so, which is unreasonable. We conclude that inhomogeneity of the tunnel current is not responsible for the experimental observations.

V. CONTROL DEVICES

A. Devices with metal instead of semiconductor

The argument used in the previous section to rule out two-step tunneling via localized interface states was based on the assumption that the states are located at the oxide/semiconductor interface, and decoupled from the semiconductor bulk bands by a Schottky barrier with resistance r_b . In principle, it is possible that the relevant localized states are present *within* the oxide tunnel barrier, and that a large spin accumulation is induced in those states by two-step tunneling. In this case the value of r_b that couples the localized states to the semiconductor bands is no longer determined by the Schottky barrier, but by the resistance of part of the tunnel oxide. It is known that two-step tunneling is more efficient for states near the center of the tunnel barrier³⁴. Hence, the associated value of r_b is determined by half of the tunnel oxide and would systematically increase with the thickness of the tunnel oxide. Depending on the parameters of the system, this could produce a spin accumulation that increases with tunnel barrier thickness, and thereby a scaling of the spin RA product with tunnel resistance.

In order to exclude this possibility, we fabricated control devices in which the semiconductor is replaced by a non-magnetic metal (Ru) electrode. If the large spin RA product originates from spin accumulation in states within the tunnel oxide, the spin accumulation does not depend on the spin resistance of the non-magnetic electrode, and a similarly large spin accumulation should be observed with a Ru metal electrode. However, in control devices with the structure Fe/MgO/Ru, no spin signal could be observed, neither Hanle nor inverted Hanle (see Fig. 5). Therefore, we conclude that the spin signal does not originate from spin accumulation in localized states in the tunnel oxide. This control experiment also rules out the recent proposal³⁵ of spin accumulation in states localized in the tunnel barrier close to the oxide/ferromagnet interface, in which a large spin accumulation is not expected to exist anyway because the strong coupling with the ferromagnet would easily deplete the spin accumulation.

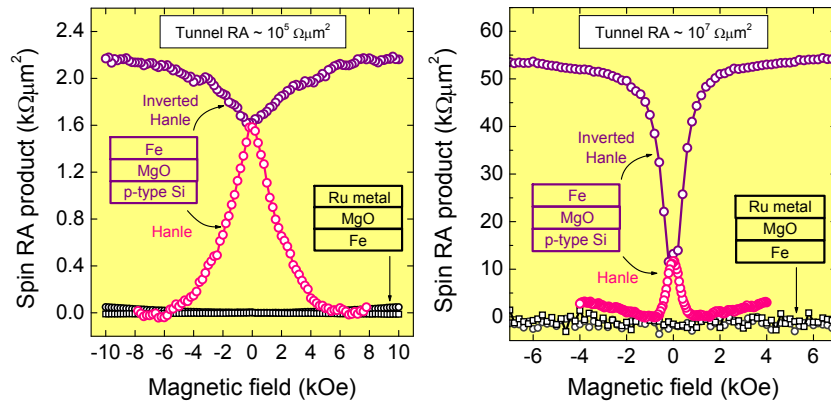


FIG. 5: Absence of spin accumulation in control tunnel devices with the Si replaced by non-magnetic Ru metal. Shown are the Hanle and inverted Hanle signal for p-type Si/MgO/Fe devices, together with similar data on control devices with Fe/MgO/Ru structure (black circles and squares). Measurements were done at 300 K, and devices with similar tunnel RA product are compared ($10^5 \Omega\mu m^2$ and $10^7 \Omega\mu m^2$ for the left and right panel, respectively). The absence of any spin signal in the metallic control devices proves the absence of spin accumulation in localized states within the MgO tunnel barrier.

B. Devices with zero tunnel spin polarization

Given that the experimental data deviates fundamentally from the theory, it is of the utmost importance to convincingly establish that the observed spin signals are genuine and originate from spin accumulation, rather than some kind of measurement artifact. Such potential artifacts can arise from (anisotropic) magnetoresistance effects related to the current through the ferromagnetic electrode itself, or from the effect of magnetic fields on charge transport in the semiconductor (Hall voltages etc.). A powerful way to exclude these artifacts is to introduce a thin non-magnetic layer at the interface between the tunnel oxide and the ferromagnet, without removing the ferromagnet⁴⁰. The method relies on the extreme interface sensitivity of (spin-polarized) tunneling, such that insertion of a thin non-magnetic layer causes the tunnel spin polarization to vanish, and hence the spin accumulation. Genuine spin signals should then disappear, whereas any signals due to artifacts, if present, would still remain. This approach was previously used to rule out artifacts in the experiments by Dash et al.^{7,41}, although only the signal for out-of plane magnetic field (Hanle curve) was investigated, and only in the range of small field. In Fig. 6, a more complete characterization is presented, showing measurements on a control device in the Hanle as well as the inverted Hanle geometry, and for fields up to 50 kOe. No spin signals are observed. This implies that the signals (Hanle and inverted Hanle) observed in the regular devices (without the non-magnetic interlayer) are not due to an artifact but originate from spin-polarized tunneling and the spin accumulation this produces. This result corroborates previous experiments on spin injection from similar ferromagnetic tunnel contacts into a silicon light emitting diode^{5,8}, from which the presence of spin-polarized carriers inside the silicon was unambiguously established.

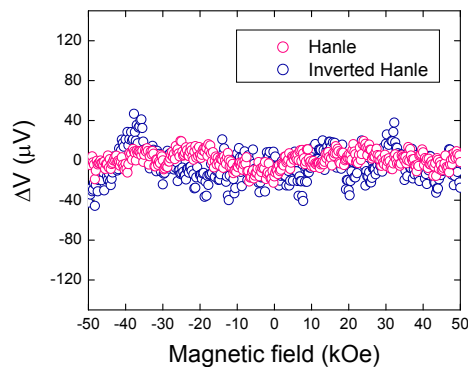


FIG. 6: Absence of spin signals in control tunnel devices with zero tunnel spin polarization. Shown are the Hanle and inverted Hanle signal for a control device with structure p-type Si/ Al_2O_3 /Au(10nm)/ $\text{Ni}_{80}\text{Fe}_{20}$, in which the non-magnetic Au interlayer causes the tunnel spin polarization to be zero. Measurements are done at room temperature with a constant current of $-195\mu\text{A}$ (hole injection condition). A constant bias voltage of about -172mV was subtracted from the data.

VI. DISCUSSION AND CONCLUSION

It has previously been noted that the magnitude of the spin accumulation signal observed in magnetic tunnel devices on semiconductors is significantly different than that predicted by the theory of spin injection, diffusion and detection, first for GaAs based devices²⁸, and subsequently also for Si and Ge based devices^{4,7}. The results presented here provide an even larger discrepancy (of up to 7 orders of magnitude), and perhaps more importantly, reveal that the scaling with tunnel barrier resistance deviates universally from theory in a fundamental way. The scaling extends over a wide range of tunnel resistance, down to the lowest tunnel RA values of about $10 \text{ k}\Omega\mu\text{m}^2$. It would certainly be of interest to extend the measurements to devices with even lower tunnel resistance. Although it was recently proposed that ferromagnetic tunnel contacts on Si with a single layer of graphene as the tunnel barrier may be ideal for this purpose^{42,43}, the obtained tunnel RA product ($6 \text{ k}\Omega\mu\text{m}^2$) was not much different from what was already achievable with oxide tunnel contacts. For instance, in silicon-based non-local devices, Fe/MgO contacts with a tunnel RA product of $4.6 \text{ k}\Omega\mu\text{m}^2$ have been successfully used for spin injection and detection by Suzuki et al.¹⁰. However, unlike the case of graphene, the oxide tunnel barriers can still be made thinner and thus appear more promising to reach even lower RA product.

Our results reveal that care has to be taken when in a particular device the observed magnitude of the spin signal is found to be in agreement with theory, because this could be accidental. For instance, the scaling trend predicts that at small junction RA product there must be a point where experiment and theory are in agreement, but a more detailed investigation varying the tunnel barrier thickness would reveal a discrepancy. This point of "accidental agreement" will shift to larger junction RA product when the thickness of the semiconductor channel is reduced, because the theory predicts a larger spin signal when the volume of semiconductor into which spins are injected is decreased. An experiment to explicitly confirm the predicted enhancement (for instance by studying devices with different channel thickness) would be helpful, but is still lacking. Clearly, one needs to look beyond the magnitude of the spin signal in order to (in)validate the theory.

While the above results are obtained with three-terminal devices and the observed signal is larger than predicted, in silicon-based non-local devices¹⁰ the observed signal deviates in the opposite direction, i.e., it is about two orders of magnitude smaller than expected, as recently noted⁴. Although in the latter case there can be several other reasons, the results presented here suggest that the difference between experiment and theory in three-terminal and non-local devices has a common origin, namely, a missing ingredient in the existing theoretical descriptions. Several explanations for the discrepancy had so far been proposed. These include two-step tunneling via localized states near the semiconductor/oxide interface²⁸, lateral inhomogeneity of the tunnel current density⁷, two-step tunneling in parallel with direct tunneling²⁹, or two-step tunneling via localized states near the oxide/ferromagnet interface³⁵. The scaling results presented here, together with the control experiments, show unambiguously that none of these proposals can explain the results. It is unclear whether the discrepancy arises from an incorrect description of the magnitude of the spin accumulation that is induced by spin injection, or from the description of the conversion of the induced spin accumulation into a voltage signal in a Hanle measurement. Obviously, resolving this puzzle is of crucial importance for application of magnetic tunnel contacts in semiconductor spintronic devices.

VII. ACKNOWLEDGEMENTS

The authors are grateful to T. Nozaki for his help with the growth of the Ru-based control devices. The authors acknowledge financial support from the Netherlands Foundation for Fundamental Research on Matter (FOM), and from the Japanese Funding Program for Next Generation World-Leading Researchers (No. GR099). One of the authors (A.S.) acknowledges a JSPS Postdoctoral Fellowship for Foreign Researchers.

Appendix A: Additional data

To investigate the effect of localized states produced by oxygen vacancies within the oxide tunnel barrier, we fabricated devices with p-type Si and Al_2O_3 tunnel barrier, but without the plasma oxidation step. Since the Al_2O_3 is grown by electron-beam deposition, the deposited oxide is oxygen deficient. We found that there is no effect on the spin signal, i.e., junctions with and without the plasma oxidation have the same spin RA product at the same tunnel resistance (Fig. 7, left panel). This suggests that two-step tunneling via localized states within the tunnel barrier plays no major role in the spin transport, consistent with the result of the control devices with Ru metal.

In order to investigate the effect of the resistance r_b of the depletion region in the Si, the Schottky barrier height was reduced (and with it r_b) using the procedure with a Cs treatment of the Si surface that was previously developed^{7,8}.

Here we present similar data as in Ref. 7 for n-type Si/ $\text{Al}_2\text{O}_3/\text{Ni}_{80}\text{Fe}_{20}$ devices with and without Cs, but now as a function of tunnel barrier thickness (Fig. 7, right panel). The Cs treatment produces no change of the spin RA product, and it scales to values of $10^6 \Omega\mu\text{m}^2$. This is not compatible with a description in terms of two-step tunneling via localized states at the oxide/Si interface. Owing to the small value of r_b for the devices treated with Cs, a large spin accumulation cannot be built up in the interface states because spins will leak away efficiently into the silicon.

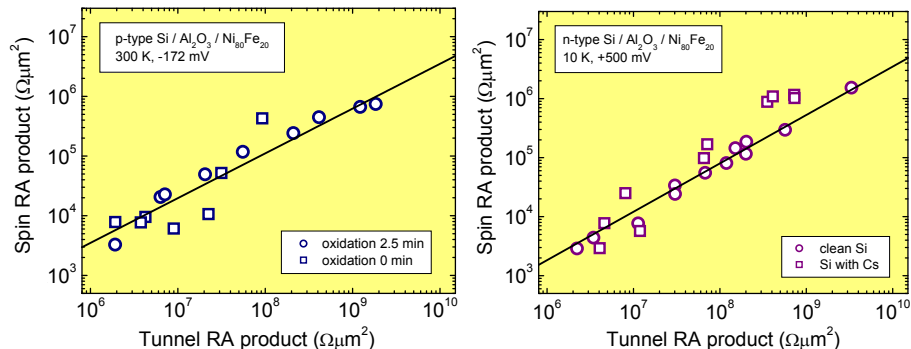


FIG. 7: Additional data on scaling of Hanle spin signals in tunnel devices with n-type and p-type Si. The open circles are the same data as in Fig. 2(b) and 2(c), whereas squares are additional data for devices with different oxidation time (p-type, left panel) and with Cs treated surfaces (n-type, right panel).

Appendix B: Hanle line width versus tunnel barrier thickness

Fig. 8 shows that the effective spin lifetime, extracted from the width of the Hanle curves, increases as a function of the tunnel resistance. For devices with an Al_2O_3 tunnel barrier, the line width is slightly dependent on the oxidation time. The spin lifetime for devices with MgO/Fe contacts is smaller than with $\text{Al}_2\text{O}_3/\text{Ni}_{80}\text{Fe}_{20}$ contacts. This is attributed to broadening of the Hanle curve by inhomogeneous magnetostatic fields, which is more pronounced for Fe owing to its larger magnetization³².

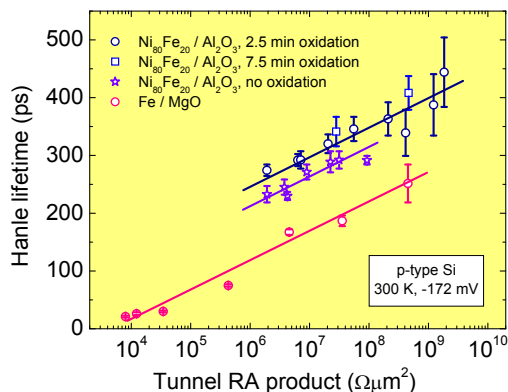


FIG. 8: Hanle line width versus tunnel resistance. The Hanle line width is characterized by an effective lifetime obtained from a fit of the Hanle curve using a Lorentzian. This time constant is a lower bound to the spin lifetime, as previously discussed^{7,23,32}. The solid lines are guides to the eye.

¹ C. Chappert, A. Fert, and F. Nguyen van Dau, *Nature Mater.* **6**, 813 (2007).

² D. D. Awschalom and M. E. Flatté, *Nature Phys.* **3**, 153 (2007).

³ A. Fert, *Rev. Mod. Phys.* **80**, 1517 (2008).

⁴ R. Jansen, *Nature Mater.* **11**, 400 (2012).

⁵ B. T. Jonker, G. Kioseoglou, A. T. Hanbicki, C. H. Li, and P. E. Thompson, *Nature Phys.* **3**, 542 (2007).

- ⁶ O. M. J. van 't Erve *et al.*, Appl. Phys. Lett. **91**, 212109 (2007).
- ⁷ S. P. Dash, S. Sharma, R. S. Patel, M. P. de Jong, and R. Jansen, Nature **462**, 491 (2009).
- ⁸ R. Jansen, B. C. Min, S. P. Dash, S. Sharma, G. Kioseoglou, A. T. Hanbicki, O. M. J. van 't Erve, P. E. Thompson, and B. T. Jonker, Phys. Rev. B **82**, 241305 (2010).
- ⁹ T. Sasaki, T. Oikawa, T. Suzuki, M. Shiraishi, Y. Suzuki, and K. Noguchi, Appl. Phys. Lett. **96**, 122101 (2010).
- ¹⁰ T. Suzuki, T. Sasaki, T. Oikawa, M. Shiraishi, Y. Suzuki, K. Noguchi, Appl. Phys. Express **4**, 023003 (2011).
- ¹¹ K. R. Jeon, B. C. Min, I. J. Shin, C. Y. Park, H. S. Lee, Y. H. Jo, and S. Ch. Shin, Appl. Phys. Lett. **98**, 262102 (2011).
- ¹² Y. Ando, K. Kasahara, K. Yamane, Y. Baba, Y. Maeda, Y. Hoshi, K. Sawano, M. Miyao, and K. Hamaya, Appl. Phys. Lett. **99**, 012113 (2011).
- ¹³ Y. Ando, Y. Maeda, K. Kasahara, S. Yamada, K. Masaki, Y. Hoshi, K. Sawano, K. Izunome, A. Sakai, M. Miyao, and K. Hamaya, Appl. Phys. Lett. **99**, 132511 (2011).
- ¹⁴ T. Inokuchi, M. Ishikawa, H. Sugiyama, Y. Saito, and N. Tezuka, J. Appl. Phys. **111**, 07C316 (2012).
- ¹⁵ M. Ishikawa, H. Sugiyama, T. Inokuchi, K. Hamaya, and Y. Saito, Appl. Phys. Lett. **100**, 252404 (2012).
- ¹⁶ H. Saito, S. Watanabe, Y. Mineno, S. Sharma, R. Jansen, S. Yuasa, and K. Ando, Solid State Comm. **151**, 1159 (2011).
- ¹⁷ Y. Zhou, W. Han, L. T. Chang, F. Xiu, M. Wang, M. Oehme, I. A. Fischer, J. Schulze, R. K. Kawakami, and K. L. Wang, Phys. Rev. B **84**, 125323 (2011).
- ¹⁸ K. R. Jeon, B. C. Min, Y. H. Jo, H. S. Lee, I. J. Shin, C. Y. Park, S. Y. Park, and S. Ch. Shin, Phys. Rev. B **84**, 165315 (2011).
- ¹⁹ A. Jain *et al.*, Appl. Phys. Lett. **99**, 162102 (2011).
- ²⁰ S. Iba, H. Saito, A. Spiesser, S. Watanabe, R. Jansen, S. Yuasa, and K. Ando, Appl. Phys. Express **5**, 023003 (2012).
- ²¹ S. Iba, H. Saito, A. Spiesser, S. Watanabe, R. Jansen, S. Yuasa, and K. Ando, Appl. Phys. Express **5**, 053004 (2012).
- ²² K. Kasahara, Y. Baba, K. Yamane, Y. Ando, S. Yamada, Y. Hoshi, K. Sawano, M. Miyao, and K. Hamaya, J. Appl. Phys. **111**, 07C503 (2012).
- ²³ R. Jansen, S. P. Dash, S. Sharma, and B. C. Min, Semicond. Sci. Technol. **27**, 083001 (2012).
- ²⁴ A. Fert and H. Jaffrès, Phys. Rev. B **64**, 184420 (2001).
- ²⁵ A. Fert, J. -M. George, H. Jaffrès, and R. Mattana, IEEE Trans. Elec. Dev. **54**, 921 (2007).
- ²⁶ S. Takahashi and S. Maekawa, Phys. Rev. B **67**, 052409 (2003).
- ²⁷ Y. Song and H. Dery, Phys. Rev. B **81**, 045321 (2010).
- ²⁸ M. Tran, H. Jaffrès, C. Deranlot, J. -M. George, A. Fert, A. Miard, and A. Lemaître, Phys. Rev. Lett. **102**, 036601 (2009).
- ²⁹ R. Jansen, A. M. Deac, H. Saito, and S. Yuasa, Phys. Rev. B **85**, 134420 (2012).
- ³⁰ B. C. Min, Ph.D. Thesis (Koninklijke Wöhrmann, Zutphen, The Netherlands, 2007). pp. 19-22.
- ³¹ A. Spiesser, S. Sharma, H. Saito, R. Jansen, S. Yuasa, and K. Ando, Proc. SPIE **8461**, 84610K (2012).
- ³² S. P. Dash, S. Sharma, J. C. Le Breton, J. Peiro, H. Jaffrès, J. -M. George, A. Lemaître, and R. Jansen, Phys. Rev. B **84**, 054410 (2011).
- ³³ J. Robertson, Rep. Prog. Phys. **69**, 327 (2006).
- ³⁴ Y. Xu, D. Ephron, and M. R. Beasley, Phys. Rev. B **52**, 2843 (1995).
- ³⁵ T. Uemura, K. Kondo, J. Fujisawa, K. Matsuda, and M. Yamamoto, Appl. Phys. Lett. **101**, 132411 (2012).
- ³⁶ S. O. Valenzuela, D. J. Monsma, C. M. Marcus, V. Narayanamurti and M. Tinkham, Phys. Rev. Lett. **94**, 196601 (2005).
- ³⁷ B. G. Park, T. Banerjee, J. C. Lodder and R. Jansen, Phys. Rev. Lett. **99**, 217206 (2007).
- ³⁸ J. Fabian, A. Matos-Abiague, C. Ertler, P. Stano, and I. Žutić, Acta Physica Slovaca **57**, 565 (2007).
- ³⁹ S. Yuasa and D. D. Djayaprawira, J. Phys. D: Appl. Phys. **40**, R337 (2007).
- ⁴⁰ R. S. Patel, S. P. Dash, M. P. de Jong, and R. Jansen, J. Appl. Phys. **106**, 016107 (2009).
- ⁴¹ S. P. Dash, S. Sharma, J. C. Le Breton, and R. Jansen, Proc. SPIE **7760**, 77600J (2010).
- ⁴² O. M. J. van 't Erve, A. L. Friedman, E. Cobas, C. H. Li, J. T. Robinson, and B. T. Jonker, Nature Nanotech. **7**, 737 (2012).
- ⁴³ H. Dery, Nature Nanotech. **7**, 692 (2012).